Review Article

Experimental animal models and evaluation techniques in intracerebral hemorrhage

Shaik Ismail Mohammed Thangameeran[a†], Cheng-Yoong Pang[a,b†], Chien-Hui Lee[c,d], Sheng-Tzung Tsai[c,d], Wei-Fen Hu[b,e], Hock-Kean Liew[b,c,e]*

[a]Institute of Medical Sciences, Tzu Chi University, Hualien, Taiwan, [b]Department of Medical Research, Hualien Tzu Chi Hospital, Buddhist Tzu Chi Medical Foundation, Hualien, Taiwan, [c]Neuro-Medical Scientific Center, Hualien Tzu Chi Hospital, Buddhist Tzu Chi Medical Foundation, Hualien, Taiwan, [d]Department of Neurosurgery, Hualien Tzu Chi Hospital, Buddhist Tzu Chi Medical Foundation, Hualien, Taiwan, [e]PhD Program in Pharmacology and Toxicology, Tzu Chi University, Hualien, Taiwan

[†]Both authors contributed equally to this work.

ABSTRACT

Intracerebral hemorrhage (ICH) is the most lethal type of cerebral stroke without effective therapy. Although clinical trials with various surgeries have been conducted, none have improved clinical outcomes compared to the current medical management for ICH. Several ICH animal models, including autologous blood injection, collagenase injection, thrombin injection, and microballoon inflation methods, have been developed to elucidate the underlying mechanisms of ICH-induced brain injury. These models could also be used for discovering new therapy for ICH preclinically. We summarize the existing ICH animal models and the evaluation parameters used to measure the disease outcomes. We conclude that these models, resembling the different aspects of ICH pathogenesis, have their advantages and disadvantages. None of the current models closely represent the severity of ICH seen in clinical settings. More appropriate models are needed to streamline ICH's clinical outcomes and be used for validating newly developed treatment protocols.

KEYWORDS: *Autologous blood injection, Collagenase injection, Intracerebral hemorrhage, Microballoon inflation*

INTRODUCTION

*I*ntracerebral hemorrhage (ICH) is the most devastating type of cerebral stroke caused by rupture of intracranial vessels or hemorrhagic transformation of cerebral infarction. Cerebral hemorrhage usually occurs in the basal ganglion, among which the nucleus (putamen) is the most common region (~50% of all cases of cerebral hemorrhage), followed by the thalamus (~15%), the pons (~15%), and the cerebellum (~10%) [1]. Moderate-to-severe disability in two-thirds of surviving ICH patients also caused an impact on the socioeconomic status of the patients and their families [2]. The prevalence of stroke in Asians is much higher than that in Westerners (20%–30% vs. 10%–15%) [3].

Our review focuses on the pathogenesis of ICH and briefing on the standard methods used to induce ICH brain injury in animals. Since rodents are the most used experimental models of ICH, our review revolves around the technical details of ICH induction and compare the similarities, differences, advantages, and disadvantages of the existing models. We also explain the evaluation methods, including magnetic resonance imaging (MRI), behavioral testing, and histological examination in these ICH animal models.

PATHOPHYSIOLOGY OF INTRACEREBRAL HEMORRHAGE

The pathogenesis of brain tissue damage caused by cerebral hemorrhage is divided into two stages: primary brain injury (PBI) and secondary brain injury (SBI) [1,4-6].

The dynamic progression and outcome of ICH are primarily influenced by hematoma expansion and perihematomal brain injury [Figure 1]. Formation of hematoma formed by hemorrhage

**Address for correspondence:* Dr. Hock-Kean Liew, Department of Medical Research, Hualien Tzu Chi Hospital, Buddhist Tzu Chi Medical Foundation, 707, Section 3, Chung-Yang Road, Hualien, Taiwan.
E-mail: hockkean@hotmail.com

Access this article online

Quick Response Code:

Website: www.tcmjmed.com
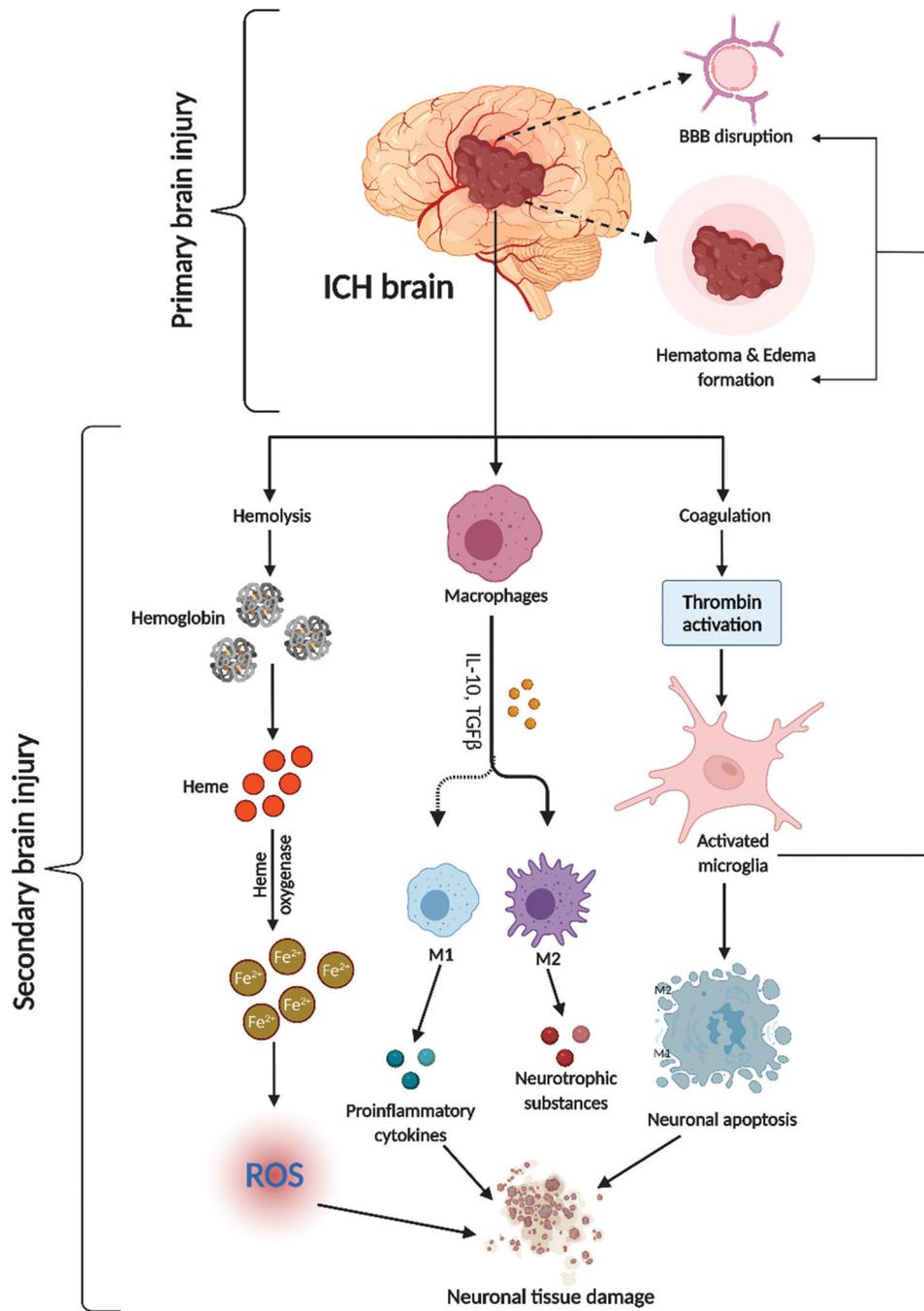
DOI: 10.4103/tcmj.tcmj_119_22

Figure 1: Pathophysiology of ICH – The primary brain injury during ICH causes the formation of hematoma and associated edema around the brain parenchyma, thereby disrupting BBB. The primary brain injury develops into a secondary brain injury as the blood components break down to release hemoglobin, heme thereby leading to excessive ROS. Simultaneously, macrophage and microglial activation also occur as part of the secondary brain injury. The macrophage differentiates into M1 (classically activated macrophage), which releases pro-inflammatory cytokines, and M2 (alternatively activated macrophage), which releases neurotrophic substances. Together with ROS, activated microglia, and M1 macrophages the secondary brain injury leads to neuronal tissue damage

after a cerebral blood vessel rupture is the primary source of PBI. Hematoma causes a mechanical impact on the brain parenchyma [2] and accelerates neurological deterioration [7]. A hematoma usually increases over time, typically around 24–48 h [2]. Hematoma and surrounding injuries cause brain edema formation and blood–brain barrier (BBB) disruption [8-11]: both events are important factors of brain injury after ICH [12,13]. Large hematoma can cause increased ICP,

reduce CPP, brain herniation, and eventually lead to death [14]. SBI of ICH is caused by the extravasated blood trigger complex and deleterious cellular and molecular consequences, including coagulation, hemolysis, and hemoglobin breakdown, which are considered the most important factor that causes brain damage after cerebral hemorrhage [3,6,15]. The coagulation cascades produce and activate the thrombin immediately in the brain after ICH, leading to activation of the microglia [Figure 1].

Microglia activation could induce BBB breaks down, early brain edema, and neuronal and glial apoptosis [16-18]. The hemolysis within hematoma usually lasts from hours to a few days and produces hemolysate that contains the hemoglobin and its breakdown products (e.g., iron, heme, and degraded heme products) [Figure 1]. These products increase the brain's reactive oxygen species (ROS), resulting in delayed edema formation and neuroinflammation [19-21].

Oxidative stress and antioxidant system in intracerebral hemorrhage

Under normal physiological conditions, the mitochondrial electron transport chain mainly generates the ROS produced by cell metabolism. Structurally and functionally complete mitochondria have a good antioxidant system, including manganese superoxide dismutase, glutathione peroxidase, catalase, glutathione reductase, heme oxygenase-1, and other enzymes. These enzymes can neutralize and metabolize ROS to maintain the balance of cell physiology [22]. Thus, cerebral hemorrhage increases ROS production and overwhelms the antioxidant defense system capacity, leading to a vicious circle that destroys mitochondrial function [23,24]. Figure 1 illustrates the pathophysiology and description.

Neuroinflammation of intracerebral hemorrhage

Inflammation after ICH is a complicated response of infiltrating immune cells, from the time of injury to the stage of healing. The primary inflammatory cells participating in inflammation include resident microglia, astrocytes, blood-derived leukocytes, and macrophage. These cells are activated and accumulated within the hemorrhagic site after ICH during SBI [Figure 1] [6]. Excessive inflammatory mediators (e.g., tumor necrosis factor-alpha, interleukin-1β [IL-1β], interferon gamma, nitric oxide synthase, intracellular adhesion molecule-1, IL-6, and matrix metalloproteinases) produced by early activation of inflammatory cells have been implicated as a possible mechanism of SBI after ICH [17,25].

Monocyte- and microglia-derived macrophage activation in intracerebral hemorrhage

"Macrophages" refer to activated myeloid cells, which can be derived either from monocytes or microglia [26-29]. Numerous studies have shown that microglia are the first responders to stroke and engage in intimate cross-talk with other intrinsic brain cells and infiltrating leukocytes that enter the brain from the peripheral through the leaky BBB [14,30-33]. In ICH, activated monocyte and microglia can differentiate into macrophage, which plays a biphasic role. They may achieve a spectrum of functional phenotypes, including the "classically activated macrophage" (M1 polarization) and the "alternative activated macrophage" (M2 polarization) [Figure 1] [31]. The M1 polarization macrophage (classical) releases a wide array of inflammatory cytokines, oxygen-free radicals, and other harmful substances during early inflammation [Figure 1]. In contrast, the M2 polarization macrophage (alternative) secretes neurotrophic substances, removes necrotic or apoptotic neuronal debris (high phagocytic activity), makes dynamic contact with neurons, and promotes the formation of glial scar tissue postinflammation [Figure 1] [31].

EXPERIMENTAL ANIMAL MODELS OF INTRACEREBRAL HEMORRHAGE

Animal models are necessary to help improve the existing therapeutic care and validate new interventions that might alleviate ICH consequences. Various animal models have been developed in practice for many years to resemble the clinical situations of ICH in humans.

Table 1 provides a description of the different experimental animal models available for ICH and the advantages and the disadvantages of the experimental animal models.

Collagenase injection

The collagenase injection model requires the injection of various amounts (0.01–0.1 units in 0.5–2 μL) of bacterial collagenase into the rat striatum. The significant advantage of this model is the high reproducibility by controlling the dosage of the bacterial collagenase, which can depict the PBI and the SBI with elevated intracranial pressure and hematoma formation followed by hematoma expansion [34]. The collagenase injection model shows hematoma increases in the first 4 h. Blood from the hemorrhagic area diffuses into the brain parenchyma after collagenase injection, increasing the hematoma volume. The hematoma volume was more significant in the collagenase injection model when compared to the blood injection model at 4 and 6 weeks [Table 1] [35].

Due to collagenase injection, it is easy to observe the time-dependent increase in the BBB leakage [35,40]. Since this model involves the formation and expansion of hematoma, toxic blood components such as free hemoglobin, heme, hemin, thrombin, and other factors affecting neurons can also be studied [Table 1]. Various studies have further probed the molecular and cellular effects caused in the brain, including neuroinflammation, neuronal death, neutrophil infiltration, and microglial activation [37].

However, the major limitation of the collagenase injection model is the significant inflammation caused by the exogenous bacterial collagenase and the rupturing of small blood vessels around the area of collagenase injection, which is not the case in clinical situations; hemorrhages in the human brain are usually from the arterial source [35]. The use of collagenase induces vessels' bursting, which results in significant bleeding even after hours of collagenase injection [10]. Maintaining the dosage of collagenase is critical in the collagenase injection model as higher dose of collagenase might induce an extensive inflammatory response causing neurotoxic effects in the animals [38]. The functional recovery of the animals can be monitored after 2 months of collagenase injection. In resemblance with the clinical outcomes of ICH, the functional neurological effects were diminished after 21 days postcollagenase injection [39-40]. Hence, this method can be used in the experimental setup as it is highly reproducible once the collagenase dose is stabilized.

Autologous blood injection

Autologous blood extracted from the tail vein infused into the striatum of the rats or mice with the help of an infusion system is closely similar to the clinical ICH [41]. The significant advantage of this model over other models is the sterility

Table 1: Experimental animal models of intracerebral hemorrhage

Models	Advantages	Disadvantages	Evaluation parameters			
			Hematoma size	Functional outcomes	BBB	Molecular and cellular effects
Collagenase injection	Highly reproducible [34]	Bacterial collagenase can amplify the inflammatory response and at high doses [34]	Hematoma size increases in the first 4 h [35]	No functional recovery was observed 21 days postcollagenase injection [36]	Time-dependent increase in the BBB permeability postcollagenase injection [35]	Presence of neutrophil after 3 days of collagenase injection [37]
			Blood from the hemorrhage site diffuses into the brain parenchyma and the hematoma volume was greater when compared to blood infusion model at 4 and 6-weeks postcollagenase injection [35]	Spontaneous functional recovery was diminished at day 1 postcollagenase injection and very minimal functional recovery was found after 2 months of collagenase injection [38,39]	BBB permeability started 30 min postcollagenase injection [40]	Dying neurons were observed as long as 21 days postcollagenase injection [37]
Autologous blood injection	Blood injection causes mechanical damage associated with mass effect [41]	Blood disruption and penetration into the subarachnoid and ventricular spaces which is unavoidable after blood injection [42]	Stable hematoma size during the first 4 h [35]	Complete functional recovery was observed after 21 days of blood injection [36]	Decreased time dependent blood–brain barrier permeability [35]	Neutrophil depletion was observed at day 3 postblood injection [37]
	Blood injection model is sterile as it does not involve any exogenous proteins [34,42]	Lack of reproducibility [43]	Hematoma resolved quickly when observed between 4 and 6 weeks [35]	Neurological severity score and corner test showed partial recovery between day 1 and day 28 postblood injection [38]	BBB permeability was observed only in the rim of the hematoma [44]	Increased number of dying neurons was found from day 2 to day 7 postblood injection [37]
Microballoon inflation	Effective in reducing the cerebral blood flow and increasing the intracranial pressure [45]	Must be performed within a limited time window to prevent irreversible brain damage [46]	Since there is no chemical disruption to disrupt tissues for bleeding to cause hematoma, this model does not induce hematoma formation [47]	No available information on the functional outcomes after microballon inflation	No BBB leakage can be traced	Microballoon inflation model causes cell death by apoptosis from 6 to 24 h after deflation [48]
	Exerted systemic effects on cerebral perfusion pressure [47]	Cannot evaluate the secondary brain injury caused by blood elements and blood brain barrier disruption [41]				Necrotic neurons were present in the microballoon inflated area in the brains of the animals for 10 or 120 min [48]
Thrombin injection	Advantageous in learning the effect of thrombin[49]	Cannot investigate other blood components other than thrombin [50]	Not considered in most of the studies as this model is used to analyze the role of thrombin	Cognitive deficit lasted for 5 days after intrastriatal injection [51]	Thrombin is said to have effects on BBB disruption in intraventricular hemorrhage [52]	Activated microglia and macrophages was observed after intrastriatal injection of thrombin [51]

BBB: Blood–brain barrier

as it does not introduce any exogenous substance. Like the collagenase model, the autologous blood injection model causes mechanical damage associated with the mass effect [41,42]. The significant disadvantages of the blood injection model are the random blood penetration into the subarachnoid and ventricular spaces [Table 1]. This model is less reproducible when compared to the collagenase model [Table 1] [32,42,43].

In terms of the hematoma size, unlike the collagenase model, which shows a constantly increasing hematoma size during the first 4 h, the blood injection model demonstrates a stable hematoma size during the first 4 h. The hematoma usually resolved as early as 4–6 weeks postblood injection [35]. The functional outcomes contrasted with the collagenase model as the animals showed complete neurological functional recovery after 21 days of blood injection. Neurological severity score and corner test showed a partial recovery from day 1 to day 28 postblood injection [36,38]. The animals which underwent blood injection ICH demonstrated deceased time-dependent

BBB permeability; also, the BBB permeability was bound only to the rim of the hematoma [35,44].

Microballoon inflation

The first microballoon inflation model was developed in 1987 to study the mass effect caused by ICH. In this model, a microballoon was inserted stereotaxically into the right caudate nucleus of rats with the help of a guided cannula, and the coordinates are as follows; 1mm cranial and 4mm to the right of bregma; the balloon was inserted into a depth of 5 mm into the brain. The microballoon (embolization balloon) was inflated with 50 μL within 20 s and was kept for 10 min before it was deflated and removed from the rat brain [45-47]. This model effectively reduced the cerebral blood flow and increased the ICP of the animals, thereby demonstrating mass effect [45]. The animals also showed systemic effects on cerebral perfusion pressure [47]. The two major disadvantages of this method are the limited time window to perform balloon inflation and an extended period of balloon inflation might result in irreversible brain damage. Another disadvantage is the lack of hematoma formation. Hence, this model cannot study the SBI caused by the blood components secreted from the hematoma and perihematomal regions [Table 1] [41,46]. Studies show that microballoon inflation causes cell death by apoptosis from 6 h to 24 h after deflation. Furthermore, necrotic neurons were present in the animals after 10 min or 120 min postdeflation [Table 1] [48].

Thrombin injection model

The model is a replica of the blood model with the only difference of injecting only thrombin and not the whole blood into the animal brain. The model differs from the blood model in that only thrombin is injected into the animal brain [Table 1]. This model's significant advantage and disadvantage are knowing the importance of thrombin and not any other blood components involved in the SBI of ICH [49,50]. However, this model showed a cognitive deficit for 5 days postthrombin injection. One further study illustrated that thrombin did not play BBB disruption [51,52]. Yang *et al.* have also shown activated microglia and macrophages after intrastriatal thrombin injection [51].

BEHAVIORAL ASSESSMENT

Standard behavioral assessment techniques evaluate rodents' neurological, motor, and sensorimotor functions from the neurological scores assessed clinically to conclude the stroke outcomes in human patients. Motor and sensorimotor analyses are carried out in an experimental setup to determine rodent stroke outcomes.

Table 2 summarizes the common techniques available for ICH evaluation in the experimental setup with the advantages and disadvantages of each techniques used.

The modified neurological severity score

The modified neurological severity score (mNSS) is the most commonly used neurological test in rodents [55]. The mNSS can be performed both for ischemic stroke and ICH, including motor, sensory, and reflex functions. The higher the score, the more severe the neurological deficit.

In most experimental brain injury models, mNSS is used to assess long-term outcomes. In ICH models, rats display a higher mNSS score as early as 1 day post-ICH, which indicates massive neurological impairment. The observational behavior of mNSS is based on the different parameters that are used in the test such as the hindlimb motor function, forelimb motor function, and body asymmetry test; mNSS is a useful tool to assess the long-term stroke outcome; and it can be used to evaluate the neuroprotective effects of novel treatments [Table 2]. The disadvantage of this method is the complexity, as it involves multiple neurological aspects. Hence, individual scores have to be taken into account to analyze the neurological deficits of specific brain regions [50,55,56].

Garcia scale

The Garcia scale was developed to assess rats' motor and sensorimotor functions [59]. In this model, the animals are tested for their motor functions with spontaneous activity (0–3), symmetry of limb movement (0–3), forelimb outstretching (0–3), climbing and grip strength (0–3), climbing and grip strength (0–3), body symmetry (0–3), and sensory function of vibrissae (0–3). The collective score is represented in the Garcia scale [Table 2]. Unlike mNSS, in the Garcia scale, high scores correspond to less neurological deficits. The significant advantage of this model is its simplicity. The Garcia scale is easy to perform, providing motor and sensorimotor functions. The major disadvantage is Garcia scale focuses more on the forelimb than the hindlimb [Table 2] [57].

Forelimb placement test

The forelimb placement test (FPT) is based on the vibrissae-elicited forelimb placing test [58]. Animals respond to vibrissae stimulation, making it easier to check ICH effects. When the animals are placed on the edge of the table, as soon as the vibrissae touch the table, normal animals will place the ipsilateral forelimb on the table, with ICH animals showing less or no response. FPT is easy to perform; however, the major disadvantage is that FPT is confined to the forelimb. It has to be combined with other neurological functional assays to assess the animals' complete motor or sensorimotor functions [Table 2] [58,59].

Open field test

An open field test was developed to assess the locomotor activity of rodents [60]. A wooden or plastic open field maze (50 cm [length] × 50 cm [width] × 38 cm [height]) is used. The animals are placed in the open field to explore for 10 min; locomotor activity is measured with the help of a video recorder. The major goal of this test is to analyze the movement of the animals placed in the chamber. With the help of video recording and automated systems, the distance, route, immobile time, and rear-up behavior can all be tracked and analyzed to evaluate the locomotor ability of the normal and ICH animals. Open field test is easy to perform and minimize human errors. The disadvantage of this method is the environmental factors that might affect the results [Table 2] [60,61].

Corner test

The corner test is used to analyze the sensorimotor and postural asymmetry [59]. The setup for the corner test is

Table 2: Common techniques for intracerebral hemorrhage evaluation in experimental setup

ICH parameters	Tests/techniques	Advantages	Disadvantages	Reference number
Behavioral assessment				
Neurological score	mNSS	Comprehensive evaluation with long term ICH outcome assessment	Can assess the neurological deficit in basal ganglia and not all parts of the brain region	[53-55]
	Garcia Scale	Easy to perform	Cannot be used for long-term neurological outcomes	[56]
Functional assay	Forelimb placement test	Easy to perform, no training required	Confined to forelimbs, not considered as a comprehensive evaluation	[57,58]
	Open field test	Easy to perform	Results will be affected due to external influences like environmental factors	[59,60]
	Corner test	Able to assess long-term neurological outcomes	Cannot be used with severely injured animals as it might affect the results	[58,61]
	Rotarod test	Able to assess long-term neurological outcomes, objective and sensitive	Training required and an experimental setup is required to perform the test	[62]
Hematoma/ lesion volume	Morphological measurements	Most common in practice, easy to perform	Animals have to be sacrificed at certain time points to get the volume of the hematoma	[55,63]
	MRI	Noninvasive and accurate	Expensive to perform	[64]
	PET/CT	Noninvasive and cost effective when compared to MRI	Combination of PET/CT scan cannot match the accuracy of anatomical and physiological features provided by a single MRI scan	[79,80]
	Cresyl violet staining	Traditionally used method to analyze the loss of neurons in a particular brain area	Not accurate	[65]
	H and E staining	Most common method used	Has to be combined with MRI to confirm the volume of the hematoma as H and E staining provides just the histopathology of the tissue	[66]
Brain water content (edema)	Dry/wet method	Easy to perform	Misinterpretation of the impact of minute changes in percentage brain water content	[67,68]
	MRI	Noninvasive, assessment of hemispheric volumes on MRI which allows a direct quantification of the space-occupied effect caused by edema formation in experimental ICH	Expensive as it involves MRI machine in the experimental setup	[69]
BBB disruption	Evans blue leakage method	Most commonly used method with a standard protocol	Potential toxicity as it is injected in vivo, free dye being present in the animal following injection	[67,68]
	FITC-dextran permeability assay	Most commonly used for quantitative studies of BBB permeability	Toxic	[64]
	Microscopic assessment	Realtime analysis of BBB disruption	Poor tissue penetration	[73-75]
	Measurement of blood proteins	No exogenous tracers required	BBB disruption cannot be analyzed at a particular time point	[75-77]
	Assessment of BBB disruption with MRI	Precision and accuracy	Needs experience to handle the machine and expensive	[75,78]

ICH: Intracerebral hemorrhage, mNSS: Modified neurological severity score, MRI: Magnetic resonance imaging, PET/CT: Positron emission tomography/computed tomography, H and E: Hematoxylin and eosin, FITC: Fluorescein isothiocyanate, BBB: Blood–brain barrier

to attach two cardboards 30 cm × 20 cm at a 30° angle. Animals are analyzed based on the side they turn upon vibrissae stimulation after placing them in the middle of the two cardboards. Able to access long-term outcomes and a practical test to analyze the sensorimotor functions post-ICH [Table 2] [59,66].

Rotarod test

The rotarod test is used to assess motor coordination. The animals are placed in a 3 cm (diameter) × 40 cm (length) rod, which rotates with the help of an electric motor. The speed of the motor increases gradually, and the latency before the animal falls is recorded. The rotarod test is sensitive as it accurately measures the motor coordination of the animals,

with a major limitation of long training trials required before the ICH surgery [Table 2] [64].

HEMATOMA/LESION VOLUME

The primary parameter measured after induction of ICH in animals is the measurement of the hematoma volume.

Morphometric measurements

Morphometric measurement is the easiest method to measure the hematoma volume after ICH in the animal model [56]. In this method, animal brains are cut coronally through the needle entry plane and serially sliced with the desired thickness. Digital photographs are taken, and the

hematoma volume is measured with the help of image analysis software [Table 2]. The major disadvantage of this method is the animals need to be sacrificed at specific time points after ICH induction [64].

Magnetic resonance imaging for hemorrhagic volume

MRI has been the most sophisticated and accurate method to measure the hematoma volume [67]. In this method, animals are anesthetized, and MRI images are captured inside the MRI machine. T2-weighted images are used to measure the hematoma volume based on the size of the hematoma. Specific software is used to measure the hematoma volume [Table 2]. MRI is the most efficient and precise method to calculate the hematoma volume; on the other hand, it is expensive and involves expertise and training to obtain the data [Table 2] [67].

Positron emission tomography/computed tomography to measure the hemorrhagic volume

The hybrid positron emission tomography/computed tomography (PET/CT) imaging can be performed to analyze the hemorrhagic volume. There are very few studies that incorporated PET/CT imagining in experimental animal models of ICH. The rats are restricted from drinking and fasting overnight before PET/CT scan in this procedure. The rats are anesthetized, and the most common radiotracer, 18F-fluorodeoxyglucose (18F-FDG), is injected via the tail vein, and the rats are allowed to rest for 30 min to ensure the uptake of 18F-FDG. The rats are then placed in the rat holder for PET imaging. Subsequently, the rats will undergo a CT scan. The hemorrhagic volume and glucose metabolism will be detected by analyzing the PET and CT images. The hybrid PET/CT is used because of the limitation of using CT, which provides us only with a detailed imagining of the brain's tissues [Table 2].

In contrast, a hybrid PET/CT scan provides images of the tissue with abnormal metabolic activity [68]. The advantages of this method are the cost-effective procedure to evaluate the hemorrhagic volume and other parameters, including glucose metabolism. This method is also noninvasive as MRI. Although hybrid PET/CT is under practice in clinical setup, MRI is preferred over CT or PET/CT in small animal research because of MRI's superior anatomic and physiological details in a single examination. This also makes the usage of MRI in small animal research more common than CT scanning [69].

BRAIN WATER CONTENT (EDEMA)

Edema is the swelling caused by the fluid trapped in the hematoma; edema is formed after the erythrocyte lysis following hematoma formation [70]. Edema can be represented by measuring the brain water content with the following two methods: dry/wet weight method and MRI.

Dry/wet weight method

In the dry/wet weight method, edema is quantified as a change in % brain water content determined from the difference between wet weights and dry weights divided by the wet weight. The brain samples are harvested from the animals and are weighed immediately to attain the wet weight.

Then, the brain samples are dried in an oven at 100°C for 24 h and weighed to obtain the dry weight. The measurement of water content can be calculated with the simple formula ([wet weight] – [dry weight]) (wet weight)$^{-1}$ × 100%. This method is simple and easy to perform with a significant disadvantage of misinterpretation of the impact of minute changes in % brain water content [71,72].

Magnetic resonance imaging for quantifying edema

MRI technique can quantify the edema or brain water content using the same approach used to determine the hematoma volume [62]. It is noninvasive, and assessing hemispheric volumes after ICH allows us to quantify the space-occupied effects of edema formation directly. Hence, further analysis can be carried out on an experimental setup of ICH. The major disadvantage is the cost and facilities required to perform the MRI edema quantification [73].

BLOOD–BRAIN BARRIER DISRUPTION

BBB disruption is a phenomenon that is regulated during the PBI of ICH. BBB leakage has been analyzed to understand the severity of the brain damage [16-18]. The following two most common methods have been used to determine the permeability of BBB in the experimental ICH models [Table 2].

Microscopic assessment

Microscopic assessment of BBB can be carried out with the help of two-photon or multiphoton microscopes where the animals are anesthetized, and craniectomy will be made on the desired cortical region. With fluorescent traces, microscopic images can be taken to analyze not just the BBB disruption, but cerebral blood flow, leukocyte behavior, and cell death can also be measured. The advantage of this model is the real-time imaging of the BBB disruption, with the major disadvantage being the poor tissue penetration [74-76].

Measurement of blood proteins

The most common method used to measure the BBB disruption is the traditional method by assessing the extravasated blood proteins from the desired brain region using immunohistochemistry or immunofluorescence analysis. This old yet reliable method is used to determine the albumin, fibrinogen, immunoglobulin M, and immunoglobulin G. There are no exogenous tracers such as Evans blue or fluorescein isothiocyanate (FITC) dextran used in this method, which is a major advantage. Time-point analysis cannot be measured with this method as the extravasation of endogenous tracers does not correspond to the BBB disruption at a particular time point, but rather a collective assessment of the blood protein extravasation from the time of injury [76-78].

Assessment of blood–brain barrier disruption with magnetic resonance imaging

MRI evaluation of BBB is a qualitative method used to measure the BBB disruption in both animals and humans. The evaluation of BBB disruption using MRI is based on the absence of contrast enhancement on the images taken from the brains of animals or humans. To obtain the MRI images of rats in the experimental setup, the rats are placed supine

on plastic support that consists of a headlock. Then, the head is inserted into the cage-like structure, which is the imaging coil. The animal is anesthetized all through this procedure. Then, MRI images are obtained in the respective planes. BBB permeability is measured with the help of injecting two boluses, the first bolus of contrast to measure the permeability and the second bolus for comparison. The advantages of this method are the accuracy of the results, with the major disadvantage being the cost and the experience needed to handle the MRI machine [76,79,80].

Evans blue leakage method

Evans blue dye has been used historically to determine the BBB permeability in various animal models [Table 2] [72]. Briefly, Evans blue dye is injected intravenously into the femoral vein of rats or mice and allowed to circulate for one hour; then, the animals undergo intracardial perfusion with normal saline. Then, the brain sections are dissected, and the fluorescence intensity of Evans blue is quantified. The major advantage of this method is its standardization, and the disadvantage is the toxicity of the Evans blue dye injection [72,73].

Fluorescein isothiocyanate-dextran

FITC-dextran is a standard method of choice for analyzing the BBB permeability. FITC-dextran is injected intravenously into the animals. Images are captured with fluorescence microscopy, and the brain capillaries and surrounding parenchyma with FITC-dextran can be analyzed to assess BBB integrity [68]. The major disadvantage is the toxicity of the FITC-dextran tracer. FITC-dextran is available in various molecular weights starting from 3 kDa to 2000 kDa for vascular outlining as the high molecular FITC-dextran gets trapped in the vessels during circulation [71].

LIMITATIONS AND CONCLUSION

It is impossible to understand ICH's molecular and cellular mechanism without a proper model. The major limitation in ICH research is the lack of a suitable animal model to mimic the clinical conditions. In the clinical setting, the volume of hematoma is larger, and the treatment protocol is formulated based on the size and position of the hematoma. With surgical treatment involving hematoma aspiration, it is important to note that the present animal models lack the similarity between the clinical severity of ICH and the treatment protocol.

There is no adequate remedy for ICH available to date. The dynamic and complicated pathophysiology process of ICH is not fully elucidated. This review provides an overview of the ICH pathophysiology, animal models used in ICH, and technical evaluation methods in practice, highlighting the advantages and disadvantages of the animal model used and the evaluation parameters.

Financial support and sponsorship

Nil.

Conflicts of interest

There are no conflicts of interest.

REFERENCES

1. Qureshi AI, Mendelow AD, Hanley DF. Intracerebral haemorrhage. Lancet 2009;373:1632-44.

2. Kazui S, Naritomi H, Yamamoto H, Sawada T, Yamaguchi T. Enlargement of spontaneous intracerebral hemorrhage. Incidence and time course. Stroke 1996;27:1783-7.

3. Qureshi AI, Tuhrim S, Broderick JP, Batjer HH, Hondo H, Hanley DF. Spontaneous intracerebral hemorrhage. N Engl J Med 2001;344:1450-60.

4. Zhou Y, Wang Y, Wang J, Anne Stetler R, Yang QW. Inflammation in intracerebral hemorrhage: From mechanisms to clinical translation. Prog Neurobiol 2014;115:25-44.

5. Xi G, Keep RF, Hoff JT. Mechanisms of brain injury after intracerebral haemorrhage. Lancet Neurol 2006;5:53-63.

6. Wang J, Doré S. Inflammation after intracerebral hemorrhage. J Cereb Blood Flow Metab 2007;27:894-908.

7. Brott T, Broderick J, Kothari R, Barsan W, Tomsick T, Sauerbeck L, et al. Early hemorrhage growth in patients with intracerebral hemorrhage. Stroke 1997;28:1-5.

8. Fenstermacher JD, Knight RA, Ewing JR, Nagaraja T, Nagesh V, Yee JS, et al. Estimating blood-brain barrier opening in a rat model of hemorrhagic transformation with Patlak plots of Gd-DTPA contrast-enhanced MRI. Acta Neurochir Suppl 2003;86:35-7.

9. Kitaoka T, Hua Y, Xi G, Hoff JT, Keep RF. Delayed argatroban treatment reduces edema in a rat model of intracerebral hemorrhage. Stroke 2002;33:3012-8.

10. MacLellan CL, Silasi G, Poon CC, Edmundson CL, Buist R, Peeling J, et al. Intracerebral hemorrhage models in rat: Comparing collagenase to blood infusion. J Cereb Blood Flow Metab 2008;28:516-25.

11. Wu J, Hua Y, Keep RF, Nakamura T, Hoff JT, Xi G. Iron and iron-handling proteins in the brain after intracerebral hemorrhage. Stroke 2003;34:2964-9.

12. Rincon F, Mayer SA. Novel therapies for intracerebral hemorrhage. Curr Opin Crit Care 2004;10:94-100.

13. Hoff JT, Xi G. Brain edema from intracerebral hemorrhage. Acta Neurochir Suppl 2003;86:11-5.

14. Keep RF, Hua Y, Xi G. Intracerebral haemorrhage: Mechanisms of injury and therapeutic targets. Lancet Neurol 2012;11:720-31.

15. Wang J. Preclinical and clinical research on inflammation after intracerebral hemorrhage. Prog Neurobiol 2010;92:463-77.

16. Wang J, Tsirka SE. Tuftsin fragment 1-3 is beneficial when delivered after the induction of intracerebral hemorrhage. Stroke 2005;36:613-8.

17. Yenari MA, Xu L, Tang XN, Qiao Y, Giffard RG. Microglia potentiate damage to blood-brain barrier constituents: Improvement by minocycline *in vivo* and in vitro. Stroke 2006;37:1087-93.

18. Lee KR, Colon GP, Betz AL, Keep RF, Kim S, Hoff JT. Edema from intracerebral hemorrhage: The role of thrombin. J Neurosurg 1996;84:91-6.

19. Wu J, Hua Y, Keep RF, Schallert T, Hoff JT, Xi G. Oxidative brain injury from extravasated erythrocytes after intracerebral hemorrhage. Brain Res 2002;953:45-52.

20. Xi G, Keep RF, Hoff JT. Pathophysiology of brain edema formation. Neurosurg Clin N Am 2002;13:371-83.

21. Huang FP, Xi G, Keep RF, Hua Y, Nemoianu A, Hoff JT. Brain edema after experimental intracerebral hemorrhage: Role of hemoglobin degradation products. J Neurosurg 2002;96:287-93.

22. Hu X, Tao C, Gan Q, Zheng J, Li H, You C. Oxidative stress in intracerebral hemorrhage: Sources, mechanisms, and therapeutic targets. Oxid Med Cell Longev 2016;2016:3215391.

23. Kim-Han JS, Kopp SJ, Dugan LL, Diringer MN. Perihematomal mitochondrial dysfunction after intracerebral hemorrhage. Stroke 2006;37:2457-62.

24. Swanson RA. Intracerebral hematoma: Beyond the mass lesion. Stroke

2006;37:2445.

25. Maier CM, Hsieh L, Crandall T, Narasimhan P, Chan PH. Evaluating therapeutic targets for reperfusion-related brain hemorrhage. Ann Neurol 2006;59:929-38.

26. Ginhoux F, Greter M, Leboeuf M, Nandi S, See P, Gokhan S, et al. Fate mapping analysis reveals that adult microglia derive from primitive macrophages. Science 2010;330:841-5.

27. Gomez Perdiguero E, Schulz C, Geissmann F. Development and homeostasis of "resident" myeloid cells: The case of the microglia. Glia 2013;61:112-20.

28. Ransohoff RM, Cardona AE. The myeloid cells of the central nervous system parenchyma. Nature 2010;468:253-62.

29. Schulz C, Gomez Perdiguero E, Chorro L, Szabo-Rogers H, Cagnard N, Kierdorf K, et al. A lineage of myeloid cells independent of Myb and hematopoietic stem cells. Science 2012;336:86-90.

30. Ahmad M, Graham SH. Inflammation after stroke: Mechanisms and therapeutic approaches. Transl Stroke Res 2010;1:74-84.

31. Benakis C, Garcia-Bonilla L, Iadecola C, Anrather J. The role of microglia and myeloid immune cells in acute cerebral ischemia. Front Cell Neurosci 2014;8:461.

32. Duan X, Wen Z, Shen H, Shen M, Chen G. Intracerebral hemorrhage, oxidative stress, and antioxidant therapy. Oxid Med Cell Longev 2016;2016:1203285.

33. Mracsko E, Veltkamp R. Neuroinflammation after intracerebral hemorrhage. Frontiers Cell Neurosci 2014;8:388.

34. Krafft PR, Rolland WB, Duris K, Lekic T, Campbell A, Tang J, et al. Modeling intracerebral hemorrhage in mice: Injection of autologous blood or bacterial collagenase. J Vis Exp 2012;67:e4289.

35. MacLellan CL, Davies LM, Fingas MS, Colbourne F. The influence of hypothermia on outcome after intracerebral hemorrhage in rats. Stroke 2006;37:1266-70.

36. Masuda T, Dohrmann GJ, Kwaan HC, Erickson RK, Wollman RL. Fibrinolytic activity in experimental intracerebral hematoma. J Neurosurg 1988;68:274-8.

37. Xue M, Del Bigio MR. Intracerebral injection of autologous whole blood in rats: Time course of inflammation and cell death. Neurosci Lett 2000;283:230-2.

38. Karki K, Knight RA, Han Y, Yang D, Zhang J, Ledbetter KA, et al. Simvastatin and atorvastatin improve neurological outcome after experimental intracerebral hemorrhage. Stroke 2009;40:3384-9.

39. Beray-Berthat V, Delifer C, Besson VC, Girgis H, Coqueran B, Plotkine M, et al. Long-term histological and behavioural characterisation of a collagenase-induced model of intracerebral haemorrhage in rats. J Neurosci Methods 2010;191:180-90.

40. Seyfried DM, Han Y, Yang D, Ding J, Shen LH, Savant-Bhonsale S, et al. Localization of bone marrow stromal cells to the injury site after intracerebral hemorrhage in rats. J Neurosurg 2010;112:329-35.

41. Manaenko A, Chen H, Zhang JH, Tang J. Comparison of different preclinical models of intracerebral hemorrhage. Acta Neurochir Suppl 2011;111:9-14.

42. Bai Q, Sheng Z, Liu Y, Zhang R, Yong VW, Xue M. Intracerebral haemorrhage: From clinical settings to animal models. Stroke Vasc Neurol 2020;5:388-95.

43. Ma Q, Khatibi NH, Chen H, Tang J, Zhang JH. History of preclinical models of intracerebral hemorrhage. Acta Neurochir Suppl 2011;111:3-8.

44. Knight RA, Han Y, Nagaraja TN, Whitton P, Ding J, Chopp M, et al. Temporal MRI assessment of intracerebral hemorrhage in rats. Stroke 2008;39:2596-602.

45. Sinar EJ, Mendelow AD, Graham DI, Teasdale GM. Experimental intracerebral hemorrhage: Effects of a temporary mass lesion. J Neurosurg 1987;66:568-76.

46. Lopez Valdes E, Hernandez Lain A, Calandre L, Grau M, Cabello A, Gomez-Escalonilla C. Time window for clinical effectiveness of mass

evacuation in a rat balloon model mimicking an intraparenchymatous hematoma. J Neurol Sci 2000;174:40-6.

47. Kingman TA, Mendelow AD, Graham DI, Teasdale GM. Experimental intracerebral mass: Description of model, intracranial pressure changes and neuropathology. J Neuropathol Exp Neurol 1988;47:128-37.

48. Nakashima K, Yamashita K, Uesugi S, Ito H. Temporal and spatial profile of apoptotic cell death in transient intracerebral mass lesion of the rat. J Neurotrauma 1999;16:143-51.

49. Xue M, Del Bigio MR. Acute tissue damage after injections of thrombin and plasmin into rat striatum. Stroke 2001;32:2164-9.

50. Xue M, Del Bigio MR. Injections of blood, thrombin, and plasminogen more severely damage neonatal mouse brain than mature mouse brain. Brain Pathol 2005;15:273-80.

51. Yang Y, Zhang M, Kang X, Jiang C, Zhang H, Wang P, et al. Thrombin-induced microglial activation impairs hippocampal neurogenesis and spatial memory ability in mice. Behav Brain Funct 2015;11:30.

52. Gao F, Liu F, Chen Z, Hua Y, Keep RF, Xi G. Hydrocephalus after intraventricular hemorrhage: The role of thrombin. J Cereb Blood Flow Metab 2014;34:489-94.

53. Lin PB, Wang PK, Pang CY, Hu WF, Tsai AP, Oblak AL, et al. Moderate ethanol pre-treatment mitigates ICH-induced injury via ER stress modulation in rats. Front Mol Neurosci 2021;14:682775.

54. Chen SF, Hsu CW, Huang WH, Wang JY. Post-injury baicalein improves histological and functional outcomes and reduces inflammatory cytokines after experimental traumatic brain injury. Br J Pharmacol 2008;155:1279-96.

55. Liew HK, Hu WF, Lin PB, Wang PK, Tsai AP, Pang CY, et al. Over-activated proteasome mediates neuroinflammation on acute intracerebral hemorrhage in rats. Cells 2019;8:E1326.

56. Khatibi NH, Ma Q, Rolland W, Ostrowski R, Fathali N, Martin R, et al. Isoflurane posttreatment reduces brain injury after an intracerebral hemorrhagic stroke in mice. Anesth Analg 2011;113:343-8.

57. Hartman R, Lekic T, Rojas H, Tang J, Zhang JH. Assessing functional outcomes following intracerebral hemorrhage in rats. Brain Res 2009;1280:148-57.

58. Hua Y, Schallert T, Keep RF, Wu J, Hoff JT, Xi G. Behavioral tests after intracerebral hemorrhage in the rat. Stroke 2002;33:2478-84.

59. Archer J. Tests for emotionality in rats and mice: A review. Anim Behav 1973;21:205-35.

60. Menard J, Treit D. Effects of centrally administered anxiolytic compounds in animal models of anxiety. Neurosci Biobehav Rev 1999;23:591-613.

61. Okauchi M, Hua Y, Keep RF, Morgenstern LB, Xi G. Effects of deferoxamine on intracerebral hemorrhage-induced brain injury in aged rats. Stroke 2009;40:1858-63.

62. Harada K, Nishimaru E, Yukutomo T, Ishida T. Detection of acute cerebral infarction by dual echo subtraction technique in MR imaging. Nihon Hoshasen Gijutsu Gakkai Zasshi 2003;59:656-62.

63. Liew HK, Pang CY, Hsu CW, Wang MJ, Li TY, Peng HF, et al. Systemic administration of urocortin after intracerebral hemorrhage reduces neurological deficits and neuroinflammation in rats. J Neuroinflammation 2012;9:13.

64. Huang LC, Liew HK, Cheng HY, Kuo JS, Hsu WL, Pang CY. Brain magnetic resonance imaging of intracerebral hemorrhagic rats after alcohol consumption. J Stroke Cerebrovasc Dis 2018;27:3493-502.

65. Zhu W, Gao Y, Chang CF, Wan JR, Zhu SS, Wang J. Mouse models of intracerebral hemorrhage in ventricle, cortex, and hippocampus by injections of autologous blood or collagenase. PLoS One 2014;9:e97423.

66. Xi G, Strahle J, Hua Y, Keep RF. Progress in translational research on intracerebral hemorrhage: Is there an end in sight? Prog Neurobiol 2014;115:45-63.

67. Saunders NR, Dziegielewska KM, Møllgård K, Habgood MD. Markers for blood-brain barrier integrity: How appropriate is Evans blue in

the twenty-first century and what are the alternatives? Front Neurosci 2015;9:385.

68. Goldim MP, Della Giustina A, Petronilho F. Using evans blue dye to determine blood-brain barrier integrity in rodents. Curr Protoc Immunol 2019;126:e83.

69. Gerriets T, Stolz E, Walberer M, Müller C, Kluge A, Bachmann A, et al. Noninvasive quantification of brain edema and the space-occupying effect in rat stroke models using magnetic resonance imaging. Stroke 2004;35:566-71.

70. Zheng H, Chen C, Zhang J, Hu Z. Mechanism and therapy of brain edema after intracerebral hemorrhage. Cerebrovasc Dis 2016;42:155-69.

71. Xu Y, He Q, Wang M, Wang X, Gong F, Bai L, et al. Quantifying blood-brain-barrier leakage using a combination of evans blue and high molecular weight FITC-Dextran. J Neurosci Methods 2019;325:108349.

72. MacLellan CL, Silasi G, Auriat AM, Colbourne F. Rodent models of intracerebral hemorrhage. Stroke 2010;41:95-8.

73. Abulrob A, Brunette E, Slinn J, Baumann E, Stanimirovic D. Dynamic analysis of the blood-brain barrier disruption in experimental stroke using time domain *in vivo* fluorescence imaging. Mol Imaging 2008;7:248-62.

74. Altay O, Suzuki H, Hasegawa Y, Caner B, Krafft PR, Fujii M, et al. Isoflurane attenuates blood-brain barrier disruption in ipsilateral hemisphere after subarachnoid hemorrhage in mice. Stroke 2012;43:2513-6.

75. Kassner A, Merali Z. Assessment of blood-brain barrier disruption in stroke. Stroke 2015;46:3310-5.

76. Schmidt-Kastner R, Meller D, Bellander BM, Strömberg I, Olson L, Ingvar M. A one-step immunohistochemical method for detection of blood-brain barrier disturbances for immunoglobulins in lesioned rat brain with special reference to false-positive labelling in immunohistochemistry. J Neurosci Methods 1993;46:121-32.

77. Jin AY, Tuor UI, Rushforth D, Kaur J, Muller RN, Petterson JL, et al. Reduced blood brain barrier breakdown in P-selectin deficient mice following transient ischemic stroke: A future therapeutic target for treatment of stroke. BMC Neurosci 2010;11:12.

78. Hoffmann A, Bredno J, Wendland M, Derugin N, Hom J, Schuster T, *et al*. MRI blood-brain barrier permeability measurements to pedict Hhemorrhagic tansformation in a rat model of ischemic stroke. Transl Stroke Res 2012;3:508-16.

79. Zhu Y, Deng L, Tang H, Gao X, Wang Y, Guo K, et al. Electroacupuncture improves neurobehavioral function and brain injury in rat model of intracerebral hemorrhage. Brain Res Bull 2017;131:123-32.

80. Psarros TG, Mickey B, Giller C. Detection of experimentally induced brain tumors in rats using high resolution computed tomography. Neurol Res 2005;27:57-9.